Appl. Phys. B (2015) 121:81–85
DOI 10.1007/s00340-015-6203-0

Applied Physics B
Lasers and Optics

Optimization of few-cycle laser pulse pumped high-order harmonic generation at 60–70 eV by changing the gas pressure

Li-Feng Wang[1] · Xin-Kui He[1] · Hao Teng[1] · Chen-Xia Yun[1] · Wei Zhang[1] · Zhiyi Wei[1]

Received: 11 March 2015 / Accepted: 10 August 2015 / Published online: 5 September 2015

Abstract We have experimentally investigated the gas cell pressure effect of high-order harmonic generation in argon and neon. The selective enhancement of high-order harmonic intensity in the energy range of 60–70 eV in the spectrum has been obtained in argon. The experimental results are simulated theoretically, and the main characterizations of the experimental observations are reproduced. By studying the ionization term effect in the simulation, we conclude that it is the plasma effect improves the phase-matching condition for this specific spectrum range and finally brings the enhancement.

1 Introduction

High-order harmonic generation (HHG) driven by the extreme nonlinear interaction between ultrafast laser pulses and atoms or molecules has shown great potential of being a novel coherent X-ray source [1] and also a source for generating attosecond pulses, which provides unprecedented tool for probing electron dynamics in rare gases, molecules, and condensed matters [2]. The physics of HHG can be clearly interpreted by classical three-step model [3], in which an electron is firstly ionized from the atomic ground state through the tunneling ionization and then accelerated by the strong laser field; at last, the electron may return to the parent ion in the oscillation of the laser field. The energy gained during the acceleration is released as a photon in the XUV range. Based on the single-electron approximation and the strong-field approximation, this simple physical picture sheds light on the state-of-art isolated attosecond pulse generation technologies, such as amplitude gating, polarization gating, double optical gating, and ionization gating [4–7].

However, the real HHG process is not happened on the single-atom level. The driving laser beam interacts with a collective of atoms in the HHG process. Each atom emits a high harmonic photon every half-cycle of the driving laser, and all generated XUV photons coherently propagate with the fundamental beam. Like other nonlinear process, phase matching is playing a critical rule for the observed XUV beam signal. Physical parameters such as the dipole phase, the Gouy phase, and the negative dispersion caused by the ionized electrons are investigated to optimize the XUV radiation [8–12]. Lu et al. [13] have experimentally observed the blueshift of the HHG spectra with 50 fs laser pulses and theoretically illustrated that the observation is due to the plasma effect. Many of these previous phase-matching studies were performed with multi-cycle driving pulse. As for isolated attosecond pulse generation, present methods always require a few-cycle driving laser. So it is very important to study the phase-matching effect of few-cycle laser driving HHG.

In this paper, the few-cycle (~5 fs) laser pulse is used to drive the HHG process. By carefully optimizing the gas pressure, the selective enhancement of the XUV emission at the energy range of 60–70 eV is obtained. We have numerically simulated the experimental process, and the results reproduce the main characterizations of the experimental spectra. We find that the plasma effect plays an important role in the observed enhancement of the XUV emission.

✉ Xin-Kui He
xinkuihe@iphy.ac.cn

✉ Zhiyi Wei
zywei@iphy.ac.cn

[1] Beijing National Laboratory for Condensed Matter Physics, Institute of Physics, Chinese Academy of Sciences, Beijing 100190, China

2 Experiments and results

A commercial Ti:sapphire amplifier (Femtopower Compact Phase, CEP) is used in the experiment, which delivers 0.8 mJ, 25 fs laser pulses at 1 kHz. The laser pulses are then focused into a 100-cm-long hollow fiber with an inner diameter of 250 μm. The fiber filled with neon is differentially pumped by filling the gas from one side and pumping out from the other side, which gives a better transmission efficiency comparing with the static pumping case [14]. The spectrum of laser pulse is broadened due to the self-phase modulation (SPM) effect, covering from 500 to 950 nm. By the combination of the chirped mirrors and the wedges, few-cycle (~5 fs) laser pulses with energy of 0.3 mJ are obtained. After that, the laser pulses are tightly focused into a gas cell filled with noble gas (argon or neon) to generate high-order harmonic emission with a 400-mm focal length silver mirror. The XUV beam is filtered by a 200-nm-thick aluminum film, which blocks the resident laser beam and diffracted by a flat-field grating. The XUV spectrum is detected by an X-ray CCD camera [15].

An argon gas cell with length of 1 mm is located after the focus in order to minimize the effect of long trajectory [16] in the experiment. Three typical experimental spectra for different gas pressures are shown in Fig. 1. The gas pressures measured in the buffer are 15.8, 13.6, and 11.5 kPa, corresponding to Fig. 1a–c, respectively. The final pressure in the gas cell is very difficult to measure. We estimate it to be 35, 30, and 26 torr, respectively, by comparing with the simulation results. We can see that the maximum photon energy recorded is around 73 eV, which is the absorption edge of aluminum. From the spatial integrated spectrum, it can be found that the results are close to the cutoff position. By increasing the gas pressure, the intensity of the harmonics increased [from (c) to (a) in Fig. 1]. For the lower order below 50 eV, we can see that the enhancement is very small. However, in the range of 60–70 eV, the HHG counts are enhanced significantly. More than three times enhancement is obtained. Also, the fine structure near 60 eV in the HHG spectrum is also dependent on the gas pressure. One thing needs to be mentioned that the minimum intensity around 53 eV in HHG spectra originates from the Cooper minimum [17] in argon. Furthermore, enhancement of the XUV emission is also observed in a 2-mm-long gas cell filled with neon. The laser parameters are the same as the case for argon. The 2-mm gas cell is used to improve the harmonic intensity in neon. In Fig. 2a–d, the gas pressure measured in the buffer is 35, 30, 25, and 18 kPa, respectively. Compared with Fig. 2b, d, the HHG intensity has been enhanced six times by increasing the gas pressure. However, the XUV radiation decreases almost one-third by comparing with Fig. 2a, b. This is originated

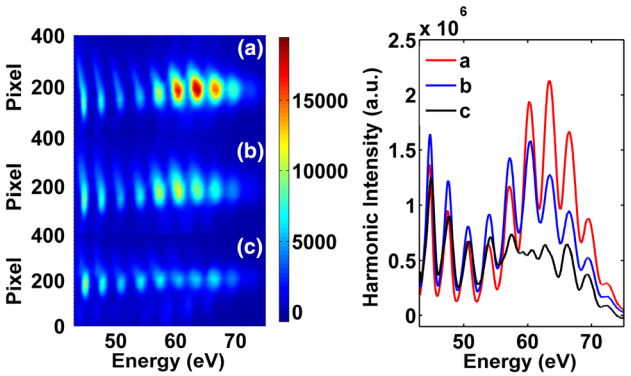

Fig. 1 Experimental spectra generated in argon for different gas pressure. *Left panel* two-dimensional spectra for three different gas pressures and *right panel* the corresponding integrated harmonic intensity

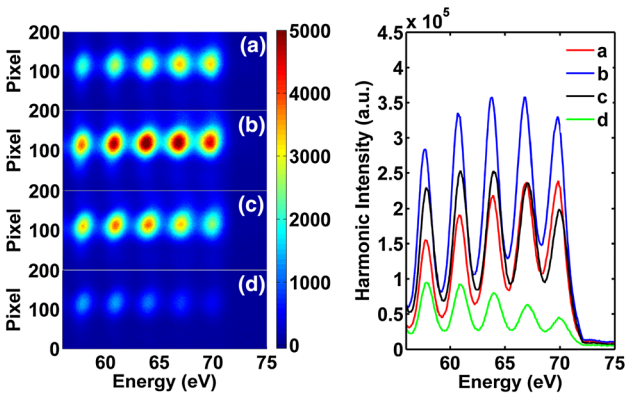

Fig. 2 Experimental spectra versus gas pressure in neon. *Left panel* two-dimensional spectra for three different gas pressures and *right panel* the corresponding integrated harmonic intensity

from the XUV absorption by the neon gas, which is studied and explained by Costant et al. [18]. The disappearance of the XUV radiation cannot be observed in our experiment because the turbo pump cannot work under the higher gas pressure. From the two figures, we can see that the tenability is much weaker comparing with the case for argon.

3 Discussion and conclusions

The feature of HHG cannot be explained by the classical three-step model. In order to reveal the physical origin of the phenomenon, we numerically solve the coupled Maxwell equations of IR laser beam and the XUV beam. In the simulation, single-atom response is calculated using the strong-field approximation method developed by Lewenstein [19], in which the nonadiabatic form of dipole moment can be written as:

$$d_{nl}(t) = 2\mathrm{Re}\left\{ i\int_{-\infty}^{t} dt' \left(\frac{\pi}{\varepsilon + i(t-t')/2}\right)^{3/2} \times E_1(t') \times d\left[p_{\mathrm{st}}(t',t) - A(t')\right] \times \exp\left[-iS_{\mathrm{st}}(t',t)\right] d^*\left[p_{\mathrm{st}}(t',t) - A(t)\right] \right\} \exp\left[-\int_{-\infty}^{t} w(t')dt'\right] \quad (1)$$

where $E_1(t)$, $A(t)$, ε, p_{st}, S_{st}, d, and $w(t)$ refer to electric field of laser pulse, vector potential, a positive regularization constant, the stationary values of the momentum, quasiclassical action, the dipole matrix element for bound-free transitions, and ionization rate, respectively. According to classic three-step model, this expression has a clear physical interpretation. First, an electron is ionized from the ground state to continuum state at time t' with the possibility amplitude $E(t') \times d\left[p_{\mathrm{st}}(t',t) - A(t')\right]$; after that, the electron accumulates a phase factor comes up to $\exp\left[-iS_{\mathrm{st}}(t',t)\right]$; at last, the electron recombines with atom at time t with an amplitude equals to $d^*\left[p_{\mathrm{st}}(t',t) - A(t)\right]$. The term of $\left(\frac{\pi}{\varepsilon+i(t-t')/2}\right)^{3/2}$ comes from the saddle-point approximation. In order to calculate the depletion of ground-state atoms in strong electric filed, ionization rate expressed as $\exp\left[-\int_{-\infty}^{t} w(t')dt'\right]$ is inserted into equation as a corrected term according the theory of Ammosov, Delone, and Krainov (ADK model) [20].

The Maxwell equation for the driving laser with single-atom response and plasma defocusing effect included is expressed as follows:

$$\nabla^2 E_1(r,z,t) - \frac{1}{c^2}\frac{\partial^2 E_1(r,z,t)}{\partial t^2} = \frac{\omega_{\mathrm{p}}^2(r,z,t)}{c^2} E_1(r,z,t) \quad (2)$$

where ω_{p} is the plasma frequency and c is the light speed in vacuum. Transformed in a moving coordinate frame ($z' = z$ and $t' = t - z/c$) and rewrite the equation in frequency domain by performing the Fourier transform, we get:

$$\nabla_{\perp}^2 \tilde{E}_1(r,z',\omega) - \frac{2i\omega}{c}\frac{\partial \tilde{E}_1(r,z',\omega)}{\partial z'} = \tilde{G}(r,z',w) \quad (3)$$

where $\tilde{E}_1(r,z',\omega) = \hat{F}\left[E_1(r,z',t')\right]$, $\tilde{G}(r,z',\omega) = \hat{F}\left[\frac{\omega_{\mathrm{p}}^2(r,z',t')}{c^2} E_1(r,z',t')\right]$, and $\hat{F}$ is the Fourier transform operator acting on the temporal coordinate. For the harmonic beam after applying the same method, the equation can be expressed in frequency domain as follows:

$$\nabla_{\perp}^2 \tilde{E}_h(r,z',\omega) - \frac{2i\omega}{c}\left(\frac{\partial}{\partial z'} + \alpha_h(\omega)\right)\tilde{E}_h(r,z',\omega) = -\omega^2 \mu_0 \tilde{P}_{nl}(r,z',\omega) \quad (4)$$

In Eq. (4), the absorption of XUV in argon is considered; α_h and μ_0 refer to the absorption coefficient of argon and permeability of vacuum. $\tilde{P}_{nl}(r,z',\omega) = \hat{F}\left[P_{nl}(r,z',t')\right]$, where $P_{nl}(r,z,t) = \left[n_0 - n_e(r,z,t)d_{nl}(r,z',t')\right]$ is the nonlinear polarization generated in the gas. Equations (3) and (4) can be numerically solved by a Crank–Nicolson routine for every frequency ω. Typical steps are 0.01 mm and 0.25 μm for the longitudinal direction and the radial direction, and 2^{11} points for 5 fs. It is worth mentioning that only one optical cycle has been taken into account in order to decrease calculation time but get reliable simulation results.

In Fig. 3a, the simulation results are shown for different gas pressures without taking into account the ionization term in argon by the strong laser field (the term calculated by the ADK model). The parameters are set at 8×10^{14} W/cm^2 for 5 fs laser pulse with wavelength of 800 nm and center of the 1 mm argon gas jet locates at 1.5 mm after the focus. The profile of the HHG spectrum is exactly the same for the three gas pressures. Even the fine structure at 80 eV is independent on the gas pressure. Also, one cannot

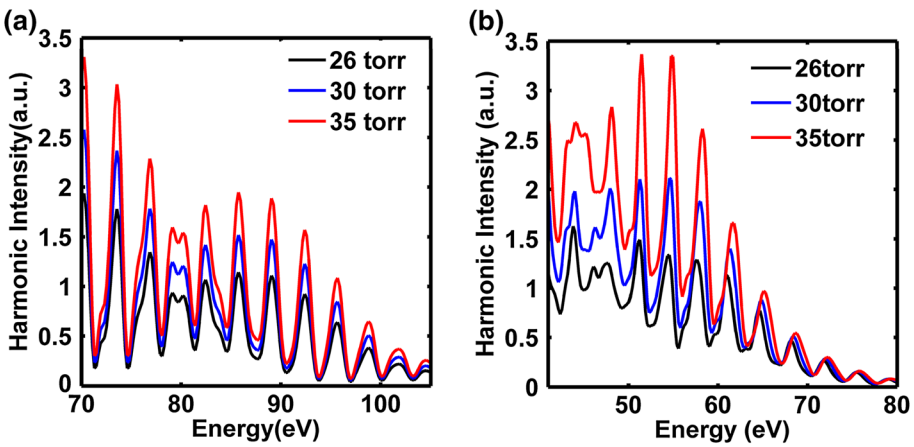

Fig. 3 Calculated HHG spectra in argon for three corresponding gas pressure without (**a**) and with (**b**) considering the ionization term in the propagation

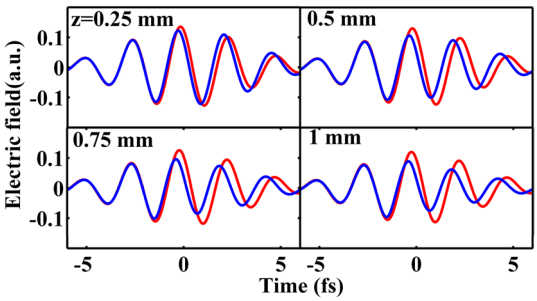

Fig. 4 Calculated electric field in time for different positions in the 1-mm gas cell. The *red* and *blue lines* are on-axis electric field calculated without and with ionization term in the propagation, respectively

find obvious enhancement of HHG intensity in the spectrum. After taking into account the plasma effect, the calculated spectra reproduce the main characterizations of the experimental spectra, as shown in Fig. 3b. First, the cutoff energy is decreased from 100 to 80 eV, comparing with Fig. 3a. Second, the HHG counts are increased predominantly in the range of 50–60 eV, just like the enhancement in the experimental spectra. Also, the fine structure at 46 eV in the spectrum changes with the gas pressure. One can get the conclusion that the plasma effect can decrease the cutoff energy, and more important, the HHG spectrum structure can be changed by the gas pressure. Enhancement of specific energy range can be obtained by optimizing the gas pressure in the HHG process.

In order to find out how the ionization in argon causes the mentioned characterizations, the on-axis electric field for three different propagation positions is shown in Fig. 4. The red and blue lines are calculated on-axis electric field without and with ionization term in the propagation, respectively. It can be found that the electric field is distorted along the propagation axis due to the interaction of ionized electrons and the laser field. In our simulation, the gas cell is located at 1.5 mm after the focus, and the total ionization rate of argon in the propagation is calculated more than 20 %. The electron ionized by the driving laser induces negative dispersion, which improves the phase-matching conditions by compensating the positive dispersion induced by noble gases. This is responsible for the predominate enhancement in Fig. 3b. However, if the ionization in argon is not considered in the simulation, the enhancement of XUV signal appears in the region of plateau and is not prominent. The ionization effect can be explained by analyzing the wave vector mismatch between the fundamental driving laser and the generated high-order harmonics in z direction, which can be wrote as: $\Delta k = q\frac{\partial \Phi_{\text{laser}}}{\partial z} + \frac{\partial \Phi_{\text{dipole}}}{\partial z} + (qk_0 - k_q)$. The first term on the right-hand side of the equation comes from the change of the laser phase through the laser focus, or more generally speaking, this term appears when the intensity of the laser is not a constant in space. The second term indicates the atomic dipole phase. It is proportional to the laser intensity, i.e., $\Phi_{\text{dipole}} \propto \alpha I_{\text{laser}}$. The third term describes the refractive difference of the fundamental and the qth-order harmonic. If the spatial mode of the driving laser is the lowest order Gaussian, the first term can be analytically wrote as Gouy phase [21] and the second term can also have an analytical expression. In our experiment, high laser intensity induces high ionization of the electron in argon, which will dramatically change the spatial distribution of the laser intensity. This process would make the first and second terms in the equation change. For example, the defocusing of the plasma will relieve the change of the laser spatially. The free electron contributes minus refractive index to the driving laser, so would change the third term in the equation. Ionization of the electron would influence all the three terms. If the parameters are proper, the total phase mismatch would be decreased and is order dependence. Our simulation and experiment verified this viewpoint that changing the pressure of the gas can optimize the phase-matching conditions for specific order of harmonic emission. Because of the spatial deformation of the laser, especially for few-cycle laser pulses, it is hard to give an analytical expression of the wave vector mismatch and separate different contributions. In order to explain the complex spatial–temporal phase-matching problem induced by the plasma, more sophisticated calculation will be further investigated.

Meanwhile, the frequency bandwidth of the on-axis laser field is dependent on the position of laser pulses in the gas cell, as shown in Fig. 5, where clear blueshift can be found. In another word, the HHG intensity is almost linear proportional to the gas pressure if the ionization term is ignored in the simulation. However, when the plasma effect due to the free-electron ionization for the laser field in the propagation is considered, the laser field intensity is decreased and the structure is reshaped. The specific spectral range

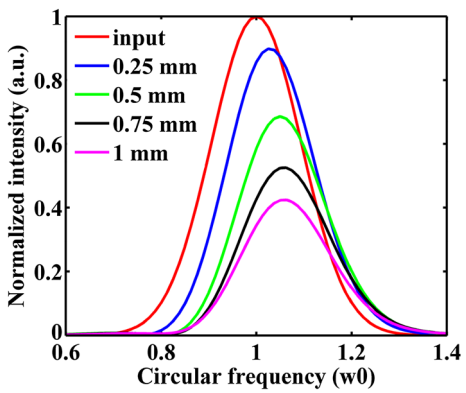

Fig. 5 Fequency bandwidth of the on-axis laser field for different positions in the 1-mm gas cell

harmonics is enhanced due to an improved phase-matching condition. It is not difficult to understand the result in Fig. 2 since the ionization rate is much lower for neon with the similar laser parameters. The enhancement at 55–72 eV in neon is almost proportional to the gas pressure.

In summary, the HHG process can be deeply understood from both microscopic and macroscopic views. In this work, the HHG spectra are investigated by tightly focusing few-cycle laser into argon and neon gas experimentally. Enhancement of the HHG intensity at 60–70 eV is observed by optimizing the gas pressure. Simulation results reproduce the main characterizations of the measured spectra by numerical solving the coupled Maxwell equations. We demonstrate that the interaction between ionized electrons and the strong laser beam is responsible for the improved XUV emission at range of 60–70 eV in argon. These finds will benefit the coherent XUV applications, such as monochromator, XUV diffraction, and FEL seed [22].

Acknowledgments The authors appreciate the fruitful discussion with Jin Chen, Bingbing Wang, Peng Ye, and Shiyang Zhong. This work was partly supported by the National Key Basic Research Program of China (Nos. 2013CB922401 and 2013CB922402), National Key Scientific Instrument and Equipment Development Projects (No. 1012YQ12004704), National Natural Science Foundation of China (Nos. 11374356 and 91126008), and the International Joint Research Program of National Natural Science Foundation of China (No. 61210017).

References

1. E. Gibson, A. Paul, N. Wagner, R. Tobey, D. Gaudiosi, S. Backus, I. Christov, A. Aquila, E. Gullikson, D. Attwood, M. Murnane, H. Kapteyn, Coherent soft X-ray generation in the water window with quasi-phase matching. Science **302**, 95 (2003)
2. F. Krausz, Misha Ivanov, Attosecond physics. Rev. Mod. Phys. **81**, 163 (2009)
3. P. Corkum, Plasma perspective on strong field multiphoton ionization. Phys. Rev. Lett. **71**, 1994 (1993)
4. M. Hentschel, R. Kienberger, Ch. Spielmann, G. Reider, N. Milosevic, T. Brabec, P. Corkum, U. Heinzmann, M. Drescher, F. Krausz, Attosecond metrology. Nature **414**, 509 (2001)
5. G. Sansone, E. Benedetti, F. Calegari, C. Vozzi, L. Avaldi, R. Flammini, L. Poletto, P. Villoresi, C. Altucci, R. Velotta, S. Stagira, S. Silvestri, M. Nisoli, Isolated single-cycle attosecond pulses. Science **314**, 443 (2006)
6. H. Mashiko, S. Gilbertson, C. Li, S.D. Khan, M.M. Shakya, E. Moon, Z. Chang, Double optical gating of high-order harmonic generation with carrier-envelope phase stabilized lasers. Phys. Rev. Lett. **100**, 103906 (2008)
7. F. Ferrari, F. Calegari, M. Lucchini, C. Vozzi, S. Stagira, G. Sansone, M. Nisoli, High-energy isolated attosecond pulses generated by above-saturation few-cycle fields. Nat. Photonics **4**, 875 (2010)
8. P. Antoine, A. L'Huillier, M. Lewenstein, Attosecond pulse trains using high-order harmonics. Phys. Rev. Lett. **77**, 1234 (1996)
9. F. Lindner, G.G. Paulus, H. Walther, A. Baltuška, E. Goulielmakis, M. Lezius, F. Krausz, Gouy phase shift for few-cycle laser pulses. Phys. Rev. Lett. **92**, 113001 (2004)
10. G. Sansone, E. Benedetti, J.P. Caumes, S. Stagira, C. Vozzi, S. De Silvestri, M. Nisoli, Control of long electron quantum paths in high-order harmonic generation by phase-stabilized light pulses. Phys. Rev. A **73**, 053408 (2006)
11. T. Ruchon, C.P. Hauri, K. Varjú, E. Mansten, M. Swoboda, R. López-Martens, A. L'Huillier, Macroscopic effects in attosecond pulse generation. New J. Phys. **10**, 025027 (2008)
12. M.B. Gaarde, J.L. Tate, K.J. Schafer, Macroscopic aspects of attosecond pulse generation. J. Phys. B At. Mol. Opt. Phys. **41**, 132001 (2008)
13. H. Lu, C. Liu, S. Zhao, P. Liu, Plasma effect on the phase matching of high harmonic generation. Chin. Opt. Lett. **9**, 011901 (2011)
14. J. Robinson, C. Haworth, H. Teng, R. Smith, J. Marangos, J. Tisch, The generation of intense, transform-limited laser pulses with tunable duration from 6 to 30 fs in a differentially pumped hollow fiber. Appl. Phys. B **85**, 525 (2006)
15. H. Teng, C. Yun, X. He, W. Zhang, L. Wang, M. Zhan, B. Wang, Z. Wei, Observation of non-odd order harmonics by sub-2-cycle laser pulses. Opt. Express **19**, 17408 (2011)
16. P. Ye, X.-K. He, H. Teng, M.-J. Zhan, S.-Y. Zhong, W. Zhang, L.-F. Wang, Z.-Y. Wei, Full quantum trajectories resolved high-order harmonic generation. Phys. Rev. Lett. **113**, 073601 (2014)
17. J. Higuet, H. Ruf, N. Thiré, R. Cireasa, E. Constant, E. Cormier, D. Descamps, E. Mével, S. Petit, B. Pons, Y. Mairesse, B. Fabre, High-order harmonic spectroscopy of the Cooper minimum in argon: experimental and theoretical study. Phys. Rev. A **83**, 053401 (2011)
18. E. Costant, D. Garzella, P. Breger, E. Mével, Ch. Dorrer, C. Le Blanc, F. Salin, P. Agostini, Optimizing high harmonic generation in absorbing gases: model and experiment. Phys. Rev. Lett. **82**, 1668 (1999)
19. M. Lewenstein, P. Balcou, M.Y. Ivanov, A. L'Huillier, P.B. Corkum, Theory of high-harmonic generation by low-frequency laser fields. Phys. Rev. A **49**, 2117 (1994)
20. E. Priori, G. Cerullo, M. Nisoli, S. Stagira, S. Silvestri, P. Villoresi, L. Poletto, P. Ceccherini, C. Altucci, R. Bruzzese, C. Lisio, Nonadiabatic three-dimensional model of high-order harmonic generation in the few-optical-cycle regime. Phys. Rev. A **61**, 063801 (2000)
21. J. Rothhardt, M. Krebs, S. Hädrich, S. Demmler, J. Limpert, A. Tünnermann, Absorption-limited and phase-matched high harmonic generation in the tight focusing regime. New J. Phys. **16**, 033022 (2014)
22. T. Togashi, E. Takahashi, K. Midorikawa, M. Aoyama, K. Yamakawa, T. Sato, A. Iwasaki, S. Owada, T. Okino, K. Yamanouchi, F. Kannari, A. Yagishita, H. Nakano, M.E. Couprie, K. Fukami, T. Hatsui, T. Hara, T. Kameshima, H. Kitamura, N. Kumagai, S. Matsubara, M. Nagasono, H. Ohashi, T. Ohshima, Y. Otake, T. Shintake, K. Tamasaku, H. Tanaka, T. Tanaka, K. Togawa, H. Tomizawa, T. Watanabe, M. Yabashi, Te Ishikawa, Extreme ultraviolet free electron laser seeded with high-order harmonic of Ti: sapphire laser. Opt. Express **19**, 317 (2011)